Title: Catalytic Effect of Ni and Cu Embedded Graphene Surface on Sulfur Dioxide (SO$_2$) Decomposition Reaction

Authors: Aykan AKÇA

Catalytic Effect of Ni and Cu Embedded Graphene Surface on Sulfur Dioxide (SO₂) Decomposition Reaction

Aykan AKÇA*[1]

Abstract

Sulfur dioxide (SO_2) decomposition reaction on Ni and Cu embedded graphene surfaces were investigated using density functional theory. Grimme-D2 correction was used for Van der Waals interactions that could be induced by the interactions between adsorbed structures and surface. Metal-embedded graphene surfaces are expected to be much cheaper than bulk system because they only use a few metal atoms contrary to bulk. Firstly, the charge density on metal embedded systems and SO_2 adsorbed on both surface was displayed with the electron density difference map and investigated with the Bader charge analysis. Then, the sequential dissociation of SO_2 were systematically investigated. Finally, SO_x molecules and their decomposed geometries were obtained and CI-NEB calculation was performed to find activation barriers related to $SO_x + yO$. It is concluded that Cu embedded graphene surface is more favorable than Ni embedded graphene surface in terms of activation energetics. Cu-based graphene materials can be used as catalyst an efficient and cheap in SO_2 decomposition.

Keywords: Nickel-embedded graphene, copper-embedded graphene, SO_2 decomposition, single-atom catalysis

1. INTRODUCTION

A significant part of energy needs in transportation, power plants, factories and houses is supplied by fossil fuels [1,2]. Sulfur dioxide (SO_2), which is an important air pollutant formed during the combustion reactions of fossil fuels, causes negative health and environmental effects known as acid rain by releasing into the atmosphere. Moreover, sulfur dioxide is an important environmental pollutant containing sulfur in its molecular structure. Environmental regulations emphasize the development of highly efficient catalysts to reduce SO_2 emissions, control automobile emissions, remove sulfur from fossil fuels, and reduce the SO_2 ratio generated during combustion reactions [3]. Adsorption and decomposition of SO_2 have been extensively studied before experimentally and theoretically on various metal surfaces including Ni [4,5] Cu [5,6], Pt [7,8], Pd [9], Rh [10]. Yokoyama et al. observed the adsorption mechanism of SO_2 on Ni (111) and Ni (100) surfaces by using near-edge-adsorption fine structure (NEXAFS) and X-ray photoelectron spectroscopy (XPS) [11]. They found that SO_2 bound to both surfaces molecularly and S-O intramolecular bonds elongated. Wilde et al. investigated the SO_2 decomposition depending on the temperature on the Ni (110) surface and they observed that SO_2 lost its molecular structure under 160 K temperature and SO_3 and S structures occurred on both surfaces [12]. Moreover, they found the average bond length of all S containing species

* Corresponding author: aykanakca@aksaray.edu.tr
[1] Aksaray University, Department of Physics, Aksaray, Turkey
ORCID: https://orcid.org/ 0000-0002-2517-765X

Aykan AKÇA

Catalytic Effect of Ni and Cu Embedded Graphene Surface on Sulfur Dioxide (SO2) Decomposition Reactio...

(S-Ni) as 2.30 Å Yokoyama et al. studied the adsorption mechanism of the SO_2 molecule on the Ni (110) surface and they reported that the S-O bond lengths elongated compared to the gas phase [13]. In another study by Jackson et al., the adsorption mechanism of SO_2 molecule on Cu (111) surface was investigated by using Chemical-shift normal-incidence X-ray standing waves (CS-NIXSW) technique [14].At that study, it was found that while SO_2 bound to the surface molecularly at low temperatures, it disintegrated as it approached to room temperature Terada et al. examined the adsorption mechanism of the SO_2 molecule on the Pd (111) surface using X-ray absorption fine structure measurements [15]. In the study, it was reported that the asymmetrical structure of SO_2 bonds played an important role in the elongation of S-O bonds Ungerer et al. investigated Platinum surface morphology and SO_2 decomposition reaction on different surfaces depending on the temperature parameter, and they stated that the percentage surface ratios expressed in Pt surface morphology changed depending on the temperature [16]. Moreover, they stated that while two surfaces ((001) and (111)) were dominant at 0 and 800 K, three surfaces ((001), (011) and (111)) were dominant at 298 and 400 K. Besides, they indicated that the Pt (111) surface was more active than other surfaces on the reaction Rodriguez et al. studied SO_2 decomposition on the surface of TiC (001) experimentally and theoretically. In their study, the adsorption heat of SO_2 was determined as 13-16 kcal/mol. Furthermore, they reported that while a significant part of the molecular structures was moving away from the surface below room temperature, some of them underwent complete decomposition into S-O atoms [17]. Rodriguez et al. investigated the catalytic activity of the Au/TiO_2 (110) surface, which was doped with metal to the metal oxide surface, on the SO_2 decomposition reaction [18]. Moreover, they reported that the Au/TiO_2 surface was more active compared to stoichiometric gold Graphene-based materials have highly superior mechanical and electrical capabilities. Because of these properties, they are used extensively in chemical sensors and catalyst researches [19-22].

To date, a few studies were available studying SO_2 decomposition on cost effective systems instead of expensive transition metals. In this study, the catalytic activities of single atom Ni and Cu elements on defective graphene substrate were theoretically investigated for SO_2 decomposition reaction.

2. COMPUTATIONAL METHODS

All calculations are by Quantum Espresso package (version 6.3, [23]) based on performed based on density functional theory GGA-PBE was selected as an exchange-correlation functional [24]. PAW (the projector augmented wave) potential was used to analyze the electronic structure [25]. 80 Ry and 800 Ry were considered for kinetic energy cutoff for wavefunctions and kinetic energy cutoff for charge density and potential, respectively during all geometric calculations. Grimme-D2 term was embedded in the system to observe the weak and van der Waals interactions [26]. $1x10^{-5}$ Ry/atom and $1x10^{-6}$ Ry/atom were used as criteria for force and energy converging during geometric optimization, respectively. Spin-polarization effect is considered for all calculations. Brillouin zone samplings of 14x14x1 for the electronic structure interactions and 4x4x1 Monkhorst-Pack k-point for geometric optimizations were used. Gas calculations were made in a 15 $Å^3$ length of three-dimensional box. Partial atomic charges were calculated by using Bader charge analysis.

The adsorption energy of atomic and molecular structures (adsorbate) on the graphene surfaces are calculated by using the following, E_{ads}, equation:

$$E_{ads}=E_{adsorbates/surface}-(E_{surface}+E_{adsorbate}) \qquad (1)$$

where $E_{adsorbates/surface}$ is the total energy of atomic and molecular system on the graphene surface; $E_{surface}$ is the total energy of the optimized graphene layer and $E_{adsorbate}$ is the total energy of the optimized atomic and molecular structures in gas phase.

Transition geometry and the energy that is needed was calculated with CI-NEB (climbing image-nudged elastic band) [27,28]. In this study, the

reaction and activation energies were calculated using the equation (2) and equation (3), respectively.

$$E_r = E_{IS} - E_{FS} \qquad (2)$$

$$E_a = E_{TS} - E_{IS} \qquad (3)$$

E_{IS} and E_{FS} represent the initial energy and final energy, respectively. E_{TS} is the transition energy between E_{IS} and E_{FS}. Avogadro [29] and Burai software [35] were used to visualize for all geometric configuration and the bond lengths.

3. RESULTS AND DISCUSSION

3.1. Modeling of Ni and Cu Embedded Graphene Surfaces

To ensure sufficient accuracy of our calculations, some important parameters obtained for Ni-embedded graphene (NiG) and Cu-embedded graphene (CuG) surfaces are given in Table 1. For modeling graphene systems, a 4×4 single-graphene layer consisting of 32 carbon atoms was constructed. The distance between the nearest C-C on the optimized graphene sheet was obtained by 1.42 Å. This value is consistent with other studies in the literature [30]. Then, the carbon at the center of graphene nanosheet were substituted with Ni or Cu. These systems are shown in Figure 1.
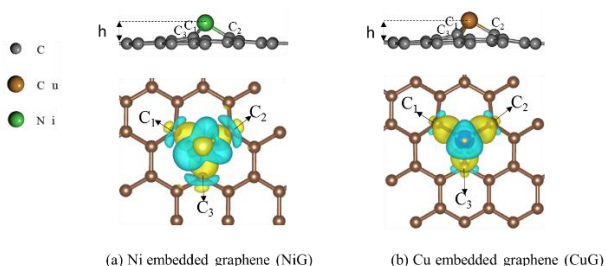

Figure 1 The electron density difference (EDD) maps (±0.006 au) of (a) Ni and (b) Cu embedded graphene systems

The binding energy of the Ni and Cu atoms to the defective graphene surface were -6.77 eV and -3.92 eV. Moreover, the bond lengths between the closest carbon atoms and Cu and Ni were 1.87 Å and 1.88 Å, respectively.

All values obtained in Table1 are consistent with the study reported by Krasheninnikov et. [31]. According to Bader charge analysis, electron transfer occurs from metal atoms to neighboring carbon atoms. After this charge transfer, positive charge accumulation is +0.67|e| and +0.65|e| at Ni and Cu atoms, respectively.

Table 1 Physical parameters obtained for the Ni and Cu embedded graphene surfaces

Parameters	NiG	CuG
Elevation-h (Å)	1.4	1.51
Bond Lengths (Å) (Ni-C), Cu-C)	1.87	1.88
Magnetic Moment (μ_B)	0	1
Binding Energy (E_B) (eV)	-6.77	-3.92
Metal (Ni, Cu), C_1, C_2, C_3 charges, |e|	+0.67,0.27,-0.22,-0.27	+0.65,0.25,-0.24,-0.20

The electron density difference (EDD) maps is plotted, where the electron density accumulation and depletion sites are displayed in yellow and blue, respectively. According to EDD, electron density accumulation was occurred around Ni-C and Cu-C bonds, which verifies strong binding between metal atom and neighboring carbon atoms. Moreover, the blue regions are showed the positive charge density around both Ni and Cu. Positive charge centers create a strong potential attraction region. Therefore, SO_2 and other intermediate state are expected to interact on these regions

3.2. The Adsorption of SO_2 on The Ni and Cu Embedded Graphene Surfaces

Two different adsorption geometry were considered for SO_2 molecule on the Cu and Ni embedded graphene surfaces. SO_2 can adsorb to graphene surfaces by both sulfur and oxygen, namely through its S-end or O-end. These configurations were showed in Figure 2 and the results obtained were given in Table 2.

In the complex_1, the adsorption energy of SO_2 was -0.9 eV on NiG surface. The bond lengths between S and O atoms were calculated to be 1.47 Å. Also, the Bader analysis reveals that about 0.34 |e| are transferred from the surface to the SO_2

Aykan AKÇA

Catalytic Effect of Ni and Cu Embedded Graphene Surface on Sulfur Dioxide (SO2) Decomposition Reactio...

molecule. According to EDD maps, a great electron density accumulation is found around the Ni-O bond, which confirms the chemical binding between the O atom and Ni. Therefore, the total electron density around the Ni Atom has been seen to decrease. In other words, very low a

charge transfer takes place from the surface to the S-O bonds. This implies that the surface has low activity over the S-O bond lengths.
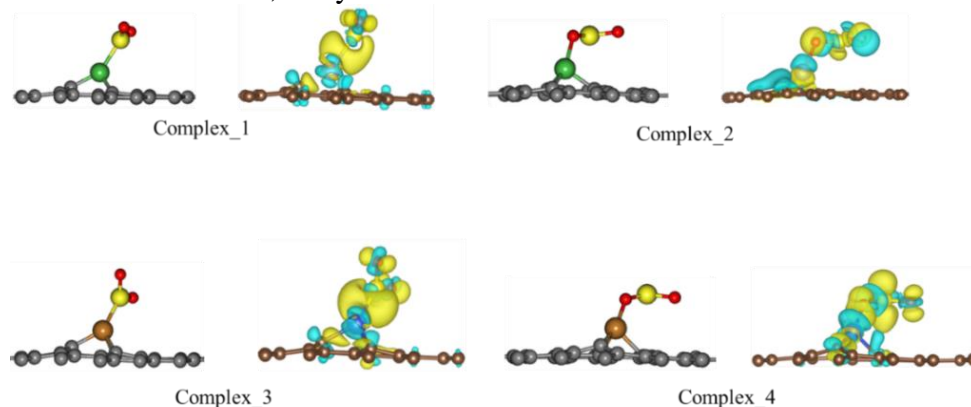

Figure 2 The different adsorption geometries of SO_2 molecules on both surface and EDD maps ($\pm$0.003 au)

Table 2 The adsorption energies and the bond lengths of SO_2 on both graphene surface and in gas phase

Bond type	NiG (Å)		CuG(Å)		Gas phase (Å)
	Complex_1	Complex_2	Complex_3	Complex_4	
S-O1	1.47	1.54	1.47	1.55	1.45
S-O2	1.47	1.48	1.47	1.49	1.45
	Eads(eV)		Eads (eV)		-
	-0.9	-1.17	-1.02	-1.36	-

In the Complex 2, the adsorption energy of the molecule SO_2, which binds to the surface by oxygen-end, is calculated as -1.17 eV. The bond lengths between S and O atoms were calculated to be 1.48 Å and 1.54 Å. Bader analysis results of these geometry showed that 0.43|e| was transferred from the surface to the SO_2 molecule. Moreover, the adsorption of the SO_2 molecule by O-end tends to cause a significant electron density on molecule, which shows elongation in the S-O bonds of the molecule.

In the Complex 3, the adsorption energy of SO_2 molecule was determined to be of -1.02 eV. Bader analysis results 0.35 |e| charge transfer was realized from the surface to the SO_2 molecule. Similar to the Bader analysis results of the "Complex 1", a great amount of electron density on Cu atom was observed to be consumed and this density was accumulated on between Cu and S. The surface had a low effect on the S-O bond length.

In the complex 4, the adsorption energy of SO_2, which is adsorbed to the surface by the O-end, is -1.36 eV. From Bader charge analysis results, a transfer of 0.47|e| from surface to SO_2 molecule was found. Most of the transferred electron was observed to accumulated on the S-O bonds. This result could be the reason for the elongation in S-O bonds that was given in Table 2.

It is found that, the adsorption geometries of SO_2, which is adsorbed to the surface by the O-end have significant catalytic activity in the elongation of S-O bonds.

3.3. Decomposition Mechanism of $SO_2 \rightarrow SO+O$ on Ni and Cu Embedded Graphene

The reaction pathway for the sequential decomposition of SO_2 to S and O on Ni and Cu embedded graphene have been systematically studied using density functional theory. The adsorption geometries of SO_2, which binds with

oxygen-end to the surfaces were considered as initial state. SO+O geometry obtained by breaking down one of the S-O bonds was considered the final geometry of first step. The transition states have been investigated using the CI-NEB method. CI-NEB method allows to calculate the energy barrier needed between the initial and final state.

For the initial state, the distance between S and O bonds was 1.48 Å, 1.54 Å and 1.49 Å, 1.55 Å on NiG and CuG, respectively. In the transition state, SO_2 molecule loses one of its oxygen bound to the sulfur atom. The oxygen atom dissociated in the TS is at distances of 2.34 Å and 1.99 Å from Sulfur atom on NiG and CuG, respectively. According to our calculations, the energy barriers required for breaking the S-O bond was 0.86 eV and 1.58 eV on NiG and CuG, respectively. The positive reaction energy values, which was found as +0.53 eV and +0.73 eV on NiG and CuG, respectively, indicates that the reaction occurred as endothermic.
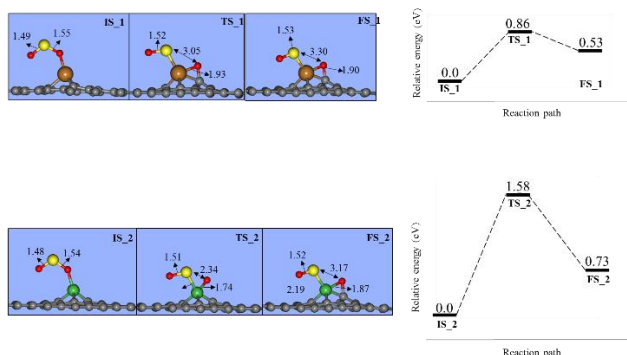

Figure 3 Side view of the initial, final, and transition states for $SO_2 \rightarrow SO+O$ on CuG ve NiG surfaces

3.4. Adsorption and Decomposition of SO molecules Ni and Cu embedded graphene surfaces

The adsorption geometry optimized of the SO molecule on both graphene surfaces was shown in Figure 4. Our calculations show that the adsorption energies of SO molecules on the Ni and Cu graphene surface were determined to be of -1.80 eV and -1.84 eV, respectively.
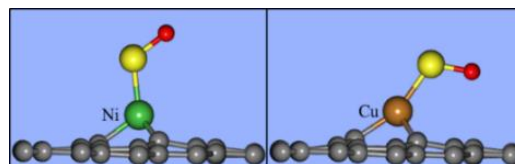

Figure 4 Side view of optimized adsorption geometries of SO molecule on CuG and NiG surfaces

The most stable adsorption geometries of the SO molecule on surfaces were considered to be the initial state of the second reaction step. The S+O configuration, which was obtained through the transition state, was considered as the final stage of the reaction. The initial, final and transition state geometries for the decomposition of SO → S+O are shown in Figure 5.
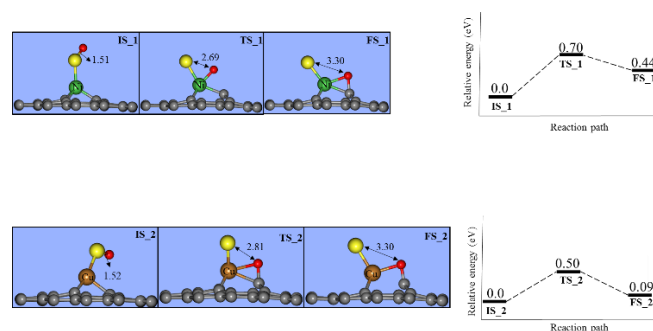

Figure 5 Side view of the initial, final and transition states for SO → S+O on CuG ve NiG surfaces.

For the initial state, the bond distances between S and O on the Ni and Cu surface was 1.51 Å and 1.52 Å. In transition state (TS), the oxygen passing over the activation energies were at distances of 2.69 Å and 2.81 Å from the sulfur atom on NiG and CuG surfaces, respectively. Moreover, the values of activation energies for NiG and CuG surfaces were calculated to be 0.70 eV and 0.50 eV, respectively. The reaction energies of SO→S+O were 0.44 eV and 0.09 eV on NiG and CuG, respectively. This reaction step occurs endothermically on both graphene surface. It also appears that the transition state geometry on the NiG surface exhibit behavior close to the IS geometry, while it was close to the FS geometry on CuG surface. This result may explain the low activation energy calculated on the CuG surface.

4. CONCLUSION

In this article, SO_2 decomposition studied on Ni and Cu embedded graphene surfaces through density functional theory. Bader charge analysis of the graphene surface was calculated and the map of electron density difference (EDD) was obtained. The charge analysis results show that a positive charge density region on the Ni and Cu atoms played an important role in detecting catalytic activity. The adsorption energies of SO_x (x= 1,2) were calculated. It was observed that SO_x structures bound to the surface through chemical interaction. The activation energies needed for the $SO_2 \rightarrow SO+O$ reaction on NiG and CuG surfaces were found as 1.58 eV and 0.86 eV, respectively. The required activation energies $SO \rightarrow S+O$ reaction were calculated as 0.70 eV for NiG and 0.50 eV for CuG. The results show that CuG surface are the more active than NiG surface. The results of the CuG surface have comparable activation barriers in all steps for other transition metals [32-34].

The Declaration of Conflict of Interest/ Common Interest

No conflict of interest or common interest has been declared by the author.

The Declaration of Ethics Committee Approval

This work does not require ethics committee permission or any special permission.

The Declaration of Research and Publication Ethics

The author of the paper declares that he complies with the scientific, ethical and quotation rules of SAUJS in all processes of the article and that he does not make any falsification on the data collected. In addition, he declares that Sakarya University Journal of Science and its editorial board have no responsibility for any ethical violations that may be encountered, and that this study has not been evaluated in any academic publication environment other than Sakarya University Journal of Science.

REFERENCES

[1]   T. Wei and B. Khoshnevis, "Integration of process planning and scheduling: a review," Journal of Intelligent Manufacturing, vol. 24, no. 6, pp. 51–63, 2000.

[2]   P. R. Buseck, and M. Pósfai, "Airborne minerals and related aerosol particles: Effects on climate and the environment," Proceedings of the National Academy of Sciences, vol. 96, no. 7, pp. 3372-3379, 1999.

[3]   A. Piéplu, O. Saur, J. C. Lavalley, O. Legendre, and C. Nédez, "Claus catalysis and H2S selective oxidation," Catalysis Reviews, vol. 40, no. 4, pp. 409-450, 1998.

[4]   X. Wei, C. Dong, Z. Chen, K. Xiao, X. Li, "Density functional theory study of SO2-adsorbed Ni (1 1 1) and hydroxylated NiO (111) surface," Applied Surface Science, vol. 355, pp. 429-435, 2015.

[5]   Y. Sakai, M. Koyanagi, K. Mogi, and E. Miyoshi, "Theoretical study of adsorption of SO2 on Ni (111) and Cu (111) surfaces," Surface Science, vol. 513, no. 2, pp. 272-282, 2002.

[6]   T. Nakahashi, S. Terada, T. Yokoyama, H. Hamamatsu, Y. Kitajima, M. Sakano, T. Ohta, "Adsorption of SO2 on Cu (100) studied by X-ray absorption fine structure spectroscopy and scanning tunneling

Aykan AKÇA

Catalytic Effect of Ni and Cu Embedded Graphene Surface on Sulfur Dioxide (SO2) Decomposition Reactio...

microscopy," Surface Science, vol. 373, no. 1, pp. 1-10, 1997.

[7] R. Streber, C. Papp, M. P. A. Lorenz, O. Höfert, E. Darlatt, A. Bayer, H. P. Steinrück, "SO2 adsorption and thermal evolution on clean and oxygen precovered Pt(111)," Chemical Physics Letters, vol. 494 no. 4-6, pp. 188-192, 2010.

[8] M. Xia, R. Yue, P. Chen, M. Wang, T. Jiao, L. Zhang, L. Li, "Density functional theory investigation of the adsorption behaviors of SO2 and NO2 on a Pt (111) surface," Colloids and Surfaces A: Physicochemical and Engineering Aspects, vol. 568, pp. 266-270, 2019.

[9] M. S. Wilburn, W. S. Epling, "SO2 adsorption and desorption characteristics of Pd and Pt catalysts: Precious metal crystallite size dependence," Applied Catalysis A: General, vol. 534, pp. 85-93, 2017.

[10] D. Fu, W. Guo, M. Li, H. Zhu, Y. Liu, "Adsorption and reaction mechanisms of SO2 on Rh (111) surface: A first-principle study," Journal of Molecular Structure, vol. 1062, pp. 68-76, 2014.

[11] T. Yokoyama, S. Terada, S. Yagi, A. Imanishi, S. Takenaka, Y. Kitajima, T. Ohta, "Surface structures and electronic properties of SO2 adsorbed on Ni (111) and Ni (100) studied by S K-edge X-ray absorption fine structure spectroscopy," Surface Science, vol. 324, no. 1, pp. 25-34, 1995.

[12] L. Wilde, M. Polcik, J. Haase, B. Brena, D. Cocco, G. Comelli, G. Paolucci "Adsorption and temperature-dependent decomposition of SO2 on Ni (110): an XPS and XAFS study," Surface Science, vol. 405, no. 2-3, pp. 215-227, 1995.

[13] T. Yokoyama, A. Imanishi, S. Terada, H. Namba, Y. Kitajima, T. Ohta, "Electronic properties of SO2 adsorbed on Ni (100) studied by UPS and O K-edge NEXAFS,"

Surface science, vol. 334, no. 1-3, pp. 88-94, 1995.

[14] G. J. Jackson, S. M. Driver, D. P. Woodruff, N. Abrams, R. G. Jones, M. T. Butterfield, V. Formoso, "A structural study of the interaction of SO2 with Cu (111)," Surface Science, vol. 459 no. 3, pp. 231-244, 2000.

[15] S. Terada, T. Yokoyama, M. Sakano, M. Kiguchi, Y. Kitajima, T. Ohta, "Asymmetric surface structure of SO2 on Pd (111) studied by total-reflection X-ray absorption fine structure spectroscopy," Chemical physics letters, vol. 300, no. 5-6, pp. 645-650, 1999.

[16] M. J. Ungerer, D. Santos-Carballal, A. Cadi-Essadek, C. G. Van Sittert, N. H. De Leeuw, "Interaction of SO2 with the Platinum (001), (011), and (111) Surfaces: A DFT Study," Catalysts, vol. 10, no. 5, pp. 558, 2020.

[17] J. A. Rodriguez, P. Liu, J. Dvorak, T. Jirsak, J. Gomes, Y. Takahashi, K. Nakamura, "Adsorption and decomposition of SO2 on TiC (0 0 1): An experimental and theoretical study," Surface Science, vol. 543, no. 1-3, pp. 675-682, 2003.

[18] J. A. Rodriguez, G. Liu, T. Jirsak, J. Hrbek, Z. Chang, J. Dvorak, A. Maiti, " Activation of gold on titania: Adsorption and reaction of SO2 on Au/TiO2 (110)," Journal of the American Chemical Society, vol. 124, no. 18, pp. 5242-5250, 2002.

[19] L. Wang, Q. Luo, W. Zhang, J. Yang, "Transition metal atom embedded graphene for capturing CO: a first-principles study," International Journal of Hydrogen Energy, vol. 39, no. 35, pp. 20190-20196, 2014.

[20] V. Singh, D. Joung, L. Zhai, S. Das, S. I. Khondaker, S. Seal, "Graphene based materials: past, present and future" Progress in Materials Science, vol. 56, no. 8, pp. 1178-1271, 2011.

[21] N.O. Weiss, H. Zhou, L. Liao, Y. Liu, S. Jiang, Y. Huang, "Graphene: an emerging electronic material" Advanced Materials, vol. 24, no. 43, pp. 5782-5825, 2012.

[22] M.R. Islam, K. Liu, Z. Wang, S. Qu, C. Zhao, X. Wang, Z. Wang, "Impact of defect and doping on the structural and electronic properties of monolayer boron phosphide," Chemical Physics, vol. 542, pp. 111054, 2021.

[23] Giannozzi P, et al. "Quantum espresso: a modular and open source software project for quantum simulations of materials," Journal of Physics: Condensed Matter, vol. 21, no. 39, pp. 395502, 2009.

[24] H. J. Monkhorst, J. D. Pack, "Special points for Brillouin-zone integrations," Physical Review B, vol. 13, no. 12, pp. 5188, 1976.

[25] G. Kresse, D. Joubert "From ultrasoft pseudopotentials to the projector augmented-wave method," Physical Review B, vol. 59, no. 3, pp. 1758, 1999.

[26] Grime S, et al. "A consistent and accurate ab initio parametrization of density functional dispersion correction (DFT-D) for the 94 elements H-Pu," The Journal of Chemical Physics, vol. 132, no. 15, pp. 154104, 2010.

[27] H. Jonsson, G. Mills, K. W. Jónsson, H. Jacobsen, W. Karsten, "Nudged elastic band method for finding minimum energy paths of transitions," 1998.

[28] G. Henkelman, B. P. Uberuaga, H. Jónsson, "A climbing image nudged elastic band method for finding saddle points and minimum energy paths," The Journal of Chemical Physics, vol. 113, no. 22, pp. 9901-9904, 2000.

[29] M. D. Hanwell, D. E. Curtis, D. C. Lonie, T. Vandermeersch, E. Zurek, G. R. Hutchison, "Avogadro: an advanced semantic chemical editor, visualization, and analysis platform," Journal of Cheminformatics, vol. 4, no. 1, pp. 1-17, 2012.

[30] O. I. Malyi, K. Sopiha, V. V. Kulish, T. L. Tan, S. Manzhos, C. Persson, "A computational study of Na behavior on graphene," Applied Surface Science, vol. 333, pp. 235-243, 2015.

[31] A. V. Krasheninnikov, P. O. Lehtinen, A. S. Foster, P. Pyykkö, R. M. Nieminen, "Embedding transition-metal atoms in graphene: structure, bonding, and magnetism," Physical review letters, vol. 102, no. 12, pp. 126807, 2009.

[32] R. Jiang, W. Guo, M. Li, H. Zhu, J. Li, L. Zhao, H. Shan, "Density functional study of the reaction of SO2 on Ir (111)," The Journal of Physical Chemistry C, vol. 113, no. 42, 18223-18232, 2009.

[33] D. Fu, W. Guo, M. Li, H. Zhu, Y. Liu, "Adsorption and reaction mechanisms of SO2 on Rh (111) surface: A first-principle study," Journal of Molecular Structure, vol. 1062, pp. 68-76, 2014.

[34] J. A. Rodriguez, J. M. Ricart, A. Clotet, F. Illas, "Density functional studies on the adsorption and decomposition of SO2 on Cu (100)," The Journal of Chemical Physics, vol. 115, no. 1, pp. 454-465, 2001.

[35] G. E. Pitti, Estudio de propiedades estructurales y electrónicas del hierro, silicio y aluminio utilizando el Software Burai (GUI de Quantum Espresso).